Mechanism and Scope of Stereospecific, Coordinative-Anionic Polymerization of Acrylamides by Chiral Zirconocenium Ester and Amide Enolates

Wesley R. Mariott and Eugene Y.-X. Chen*

Department of Chemistry, Colorado State University, Fort Collins, Colorado 80523-1872

Received May 24, 2005; Revised Manuscript Received May 27, 2005

ABSTRACT: The mechanism and scope of the isospecific, coordinative-anionic polymerization of acrylamides, including *N,N*-dimethylacrylamide (DMAA), *N,N*-dimethylmethacrylamide (DMMA), and *N*-isopropylacrylamide (IPAA), using chiral *ansa*-zirconocenium ester and amide enolates, are reported. The zirconocenium ester enolate, *rac*-(EBI)Zr^+(THF)[OC(O^{i}Pr)═CMe_2][$MeB(C_6F_5)_3$]$^-$ [**1**; EBI = $C_2H_4(Ind)_2$], effects highly isospecific and living polymerization of DMAA via a monometallic, intramolecular coordinative-conjugate-addition mechanism, with the resting intermediate during a "catalytic" propagation cycle being the cyclic amide enolate. The results leading to these key conclusions were derived from investigations of polymerization kinetics, polymer microstructures and chain-end groups, and block copolymerization behavior as well as modeling and isolation of the active propagating species. Specifically regarding the active species modeling, isolation, and characterization, neutral chiral amide enolate *rac*-(EBI)ZrMe[$OC(NMe_2)$═CMe_2] (**2**) has been synthesized and structurally characterized and its corresponding cationic complex *rac*-(EBI)Zr^+(THF)[$OC(NMe_2)$═$C(Me)_2$][$MeB(C_6F_5)_3$]$^-$ (**3**) isolated; cation **3** is highly active for DMAA polymerization, serving as a structural model for the active propagating species. Both ester and amide enolates **1** and **3** are inactive for polymerizations of DMMA and IPAA; however, 1 equiv of IPAA or DMMA is readily added to **1** or **3**, forming the eight-membered-ring cyclic amide enolates *rac*-(EBI)Zr^+[$OC(NH^iPr)$═$CHCH_2C(Me_2)C(O^iPr)$═O][$MeB(C_6F_5)_3$]$^-$ (**4**) or *rac*-(EBI)Zr^+[$OC(NMe_2)$═$C(Me)$-$CH_2C(Me_2)C(NMe_2)$═O][$MeB(C_6F_5)_3$]$^-$ (**5**), which correspond to the structures of the first acrylamide addition products and the resting propagation intermediates.

Introduction

An important yet still challenging goal in polymerizations of many prochiral, functionalized vinyl monomers is to achieve a high degree of control over the stereochemistry of the polymerization of such monomers. One example in this context is the polymerization of *N,N*-dimethylacrylamide (DMAA); both anionic and radical polymerizations of DMAA with initiators (and additives) that can promote tacticity control yielded poly(*N,N*-dimethylacrylamide) [P(DMAA)] with only moderate isotacticities {[*mm*] = 54−81%}.[1−6] Butler and co-workers first reported the polymerization of DMAA using an anionic initiator (EtLi) in toluene, affording crystalline isotactic P(DMAA);[1] the crystalline P(DMAA) produced by *s*-BuLi was later analyzed by McGrath et al. using ^{1}H and ^{13}C NMR and was shown to exhibit an isotacticity of ∼81%.[2] Xie and Hogen-Esch found that the P(DMAA) produced by Ph_3CLi or ($Ph_2CCH_2CH_2$-CPh_2)Li_2 in THF at −78 °C was also isotactic-rich ([*mm*] = 54%).[3] Nakahama and co-workers used anionic initiators modified with Lewis acids such as Et_2Zn and Et_3B to effect the tacticity of the resulting P(DMAA);[4] they found that the presence of such Lewis acid additives typically reduces the P(DMAA) isotacticity and thus enhances the syndioselectivity of anionic polymerization. The trend is reversed, however, for radical polymerizations where Lewis acids such as $M(OTf)_3$ (M = Y, Sc, Yb) are shown to enhance isotacticity of the polymer, as demonstrated by the work of Okamoto and co-workers.[5] Most recently, Matyjaszewski et al. utilized this Lewis acid effect to synthesize atactic-*b*-isotactic stereoblock P(DMAA) by adding $Y(OTf)_3$ at a given time to an atom-transfer radical polymerization (ATRP) of DMAA, initially started without the Lewis acid.[6]

Recognizing the difficulty and complications in achieving high degrees of stereochemical control over the polymerization of acrylamides using anionic or radical initiators, we recently explored the possibility of accomplishing this goal using a coordination polymerization mediated by chiral *ansa*-metallocenium complexes.[7] A large number of investigations have been directed toward studies of the polymerization of alkyl methacrylates, especially methyl methacrylate (MMA), by group 4 metallocene and related complexes, including achiral zirconocenes,[8] chiral *ansa*-zirconocenes,[9] achiral titanocenes,[10] chiral *ansa*-titanocenes,[11] half-sandwich titanium complexes,[12] and constrained geometry titanium and zirconium complexes;[13] the polymerization of MMA by zirconocenes has also been examined computationally.[14] Despite these major advances in the polymerization of *methacrylates* using group 4 metallocene complexes, it is significant to note here that, to the best of our knowledge, there is only *one* open publication on the polymerization of *acrylamides* using metallocene complexes,[7] in which we communicated the isospecific coordination polymerization of DMAA. Using this polymerization mediated by the well-defined, isolated chiral *ansa*-zirconocenium ester enolate complex, *rac*-(EBI)Zr^+(THF)[OC(O*i*Pr)═CMe_2][$MeB(C_6F_5)_3$]$^-$ [**1**; EBI = $C_2H_4(Ind)_2$], we synthesized P(DMAA) with unprecedented isotacticity ([*mm*] > 99%).

In our continuing studies of the polymerization of acrylamides using chiral *ansa*-zirconocenium complexes, we focus here on the mechanism and scope of this polymerization and present a full account of our efforts to better understand the polymerization control, ste-

* Corresponding author. E-mail: eychen@lamar.colostate.edu.

10.1021/ma051061q CCC: $30.25
Published on Web 07/02/2005

reoregulation, comonomer selectivity, active species, and kinetics, utilizing two complementary initiating complex structures, chiral *ansa*-zirconocenium *ester* enolate complex **1**, and chiral *ansa*-zirconocenium *amide* enolate complex *rac*-(EBI)Zr^+(THF)[OC(NMe_2)=C($Me)_2$][MeB($C_6F_5)_3$]$^-$ (**3**). Key findings of this study include (a) the living polymerization of DMAA by **1** proceeds via a monometallic, coordinative conjugate addition mechanism; (b) sequential block copolymerization of MMA and DMAA leads to the formation of the well-defined, highly isotactic block copolymer P(MMA)-*b*-P(DMMA), with a procedure starting from the MMA polymerization, but not starting from the DMAA polymerization; (c) neither complex **1** nor **3** is active for the polymerization of *N,N*-dimethylmethacrylamide (DMMA) or *N*-isopropylacrylamide (IPAA), but 1 equiv of IPAA or DMMA can be readily added to **1** or **3**, forming the corresponding single-monomer-addition products—eight-membered-ring cyclic amide enolate complexes; and (d) polymerization of DMAA by **3** proceeds in a manner similar to that by **1**, indicating that the amide enolate **3** is a suitable structural model for the active propagating species derived from the polymerization acrylamides.

Experimental Section

Materials and Methods. All syntheses and manipulations of air- and moisture-sensitive materials were carried out in flamed Schlenk-type glassware on a dual-manifold Schlenk line, a high-vacuum line (10^{-5}−10^{-7} Torr), or in an argon-filled glovebox (typically <1.0 ppm oxygen and moisture). NMR-scale reactions (typically in a 0.02 mmol scale) were conducted in Teflon-valve-sealed J. Young-type NMR tubes. HPLC grade organic solvents were sparged with nitrogen during filling of the solvent reservoir and then dried by passage through activated alumina (for Et_2O, THF, and CH_2Cl_2) followed by passage through Q-5-supported copper catalyst (for toluene and hexanes) stainless steel columns. Benzene-d_6, toluene-d_8, and THF-d_8 were dried over sodium/potassium alloy and vacuum-distilled or filtered, whereas C_6D_5Br, $CDCl_3$, CD_2Cl_2, and *o*-dichlorobenzene were dried over activated Davison 4 Å molecular sieves. NMR spectra were recorded on either a Varian Inova 300 (FT 300 MHz, ^{1}H; 75 MHz, ^{13}C; 282 MHz, ^{19}F) or a Varian Inova 400 spectrometer. Chemical shifts for ^{1}H and ^{13}C spectra were referenced to internal solvent resonances and are reported as parts per million relative to tetramethylsilane, whereas ^{19}F NMR spectra were referenced to external $CFCl_3$. Elemental analyses were performed by Desert Analytics, Tucson, AZ.

Diisopropylamine, triflic acid, *n*-butyllithium (1.6 M in hexanes), *N,N*-dimethylisobutyramide, lithium dimethylamide, and tetrachlorozirconium were purchased from Aldrich Chemical Co. and used as received, except for the amine and the amide which were degassed using three freeze−pump−thaw cycles. Trimethylaluminum (neat) was purchased from Strem Chemical Co. and methyllithium (1.6 M in diethyl ether) from Acros. 2,6-Di-*tert*-butyl-4-methylphenol (butylated hydroxytoluene, BHT-H) was purchased from Aldrich Chemical Co. and recrystallized from hexanes prior to use.

Methyl methacrylate (MMA) was purchased from Aldrich Chemical Co., whereas *N,N*-dimethylacrylamide (DMAA), *N,N*-dimethylmethacrylamide (DMMA), and *N*-isopropylacrylamide (IPAA) were purchased from TCI America. MMA, DMAA, and DMMA were first degassed and dried over CaH_2 overnight, followed by vacuum distillation; final purification of MMA involved titration with neat tri(*n*-octyl)aluminum to a yellow end point[15] followed by distillation under reduced pressure. The purified monomers were stored in brown bottles over activated Davison 4 Å molecular sieves (for DMAA and DMMA) in a −30 °C freezer inside the glovebox. IPAA was recrystallized from a toluene/hexanes solvent mixture and stored in a −30 °C freezer inside the glovebox.

Tris(pentafluorophenyl)borane, B($C_6F_5)_3$, was obtained as a research gift from Boulder Scientific Co. and further purified by recrystallization from hexanes at −35 °C. The ($C_6F_5)_3$B·THF adduct was prepared by addition of THF to a toluene solution of the borane followed by removal of the volatiles and drying in vacuo. Literature procedures were employed for the preparation of the following compounds and metallocene complexes: (EBI)H_2 [EBI = C_2H_4(Ind)$_2$],[16] *rac*-(EBI)Zr($NMe_2)_2$,[17] *rac*-(EBI)ZrMe_2,[17] *rac*-(EBI)ZrMe^+Me(B$(C_6F_5)_3$)$^-$ (M = B, Al),[18,9a] *rac*-(EBI)Zr(OTf)$_2$,[9a] *rac*-(EBI)ZrMe(OTf),[9a] *rac*-(EBI)ZrMe[OC(O^{i}Pr)=CMe_2],[9a] and *rac*-(EBI)Zr^+(THF)[OC(O^{i}Pr)=CMe_2][MeB($C_6F_5)_3$]$^-$ (**1**).[9a] The lithium amide enolate LiOC(NMe_2)=CMe_2 was prepared according to a modified literature procedure of Rathke and co-workers.[19]

Synthesis of *rac*-(EBI)ZrMe[OC(NMe_2)=CMe_2] (2). In an argon-filled glovebox, a 30 mL glass reactor was equipped with a magnetic stir bar, charged with 20 mL of toluene, and cooled to −30 °C. To this prechilled reactor, with vigorous stirring, was added 0.30 g (0.58 mmol) of *rac*-(EBI)ZrMe(OTf) followed by addition of 0.07 g (0.58 mmol) of lithium amide enolate LiOC(NMe_2)=CMe_2. The resulting suspension was stirred for 1 day at ambient temperature, after which it was filtered through a pad of Celite. The solvent of the filtrate was removed in vacuo, yielding 0.27 g (96%) of the spectroscopically pure **2** as a yellow powder. Anal. Calcd for $C_{27}H_{31}NOZr$: C, 68.02; H, 6.55; N, 2.94. Found: C, 67.75; H, 6.51; N, 2.89.

^{1}H NMR (C_6D_6, 23 °C) for **2**: δ 7.42 (d, J = 9.2 Hz, 1H), 7.18−6.80 (m, 7H), 6.37 (d, J = 3.2 Hz, 1H), 6.14 (d, J = 3.2 Hz, 1H), 5.83 (d, J = 3.2 Hz, 1H), 5.62 (d, J = 3.2 Hz, 1H), 3.20−2.80 (m, 4H, CH_2CH_2), 2.22 (s, 6H, NMe_2), 1.91 (s, 3H, =CMe_2), 1.31 (s, 3H, =CMe_2), −0.53 (s, 3H, ZrCH_3). ^{13}C NMR (C_6D_6, 23 °C): δ 156.42 [O*C*(NMe$_2$)=], 127.70, 126.77, 125.95, 124.97, 124.71, 124.55, 124.29, 123.24, 122.76, 121.93, 121.18, 118.94, 115.86, 114.33, 111.38, 105.10, 102.97, 95.54 (18 resonances for indenyl-ring carbons), 95.14 (=*C*Me$_2$), 42.48 (N*Me*$_2$), 30.68 (Zr*C*H$_3$), 28.39 (*C*H$_2$CH$_2$), 27.60 (CH$_2$*C*H$_2$), 19.10 (=C*Me*$_2$), 18.68 (=C*Me*$_2$).

Synthesis of *rac*-(EBI)Zr^+(THF)[OC(NMe_2)=CMe_2][MeB($C_6F_5)_3$]$^-$ (3). In an argon-filled glovebox, a 30 mL glass reactor was equipped with a magnetic stir bar, charged with 100 mg (0.210 mmol) of **2**, 123 mg (0.210 mmol) of ($C_6F_5)_3$B·THF, and 5 mL of CH_2Cl_2. The resulting dark red solution was allowed to stir for 20 min at ambient temperature before the solvent was removed in vacuo, affording a sticky orange-red residue. This residue was washed with 3 × 2 mL of hexanes and dried under vacuum for 2 h, yielding 214 mg (96%) of the analytically pure title compound as an orange-red powder. Anal. Calcd for $C_{49}H_{39}BF_{15}NO_2Zr$: C, 55.48; H, 3.71; N, 1.32. Found: C, 55.74; H, 4.00; N, 1.38.

^{1}H NMR (CD_2Cl_2, 23 °C) for **3**: δ 8.12 (d, J = 8.4 Hz, 1H), 7.95 (d, J = 8.8 Hz, 1H), 7.50−7.16 (m, 6H), 6.31 (m, 2H), 6.23 (m, 2H), 4.12 (m, 2H, CH_2CH$_2$), 3.85 (m, 2H, CH$_2$CH_2), 3.76 (s, br, 2H, α-CH_2, THF), 3.46 (s, br, 2H, α-CH_2, THF), 2.38 (s, 6H, NMe_2), 2.04 (s, br, 2H, β-CH_2, THF), 1.88 (s, br, 2H, β-CH_2, THF), 1.51 (s, 3H, −CMe_2), 1.40 (s, 3H, −C*Me*$_2$), 0.51 (s, br, 3H, BCH_3). ^{19}F NMR (CD_2Cl_2, 23 °C): δ −131.50 (d, $^3J_{F-F}$ = 24.3 Hz, 6F, *o*-F), −163.51 (t, $^3J_{F-F}$ = 18.4 Hz, 3F, *p*-F), −166.13 (t, $^3J_{F-F}$ = 18.4 Hz, 6F, *m*-F). ^{13}C NMR (CD_2Cl_2, 23 °C): δ 155.83 [O*C*(NMe$_2$)=], 148.83 (d, $^1J_{C-F}$ = 238.4 Hz, C_6F_5), 138.03 (d, $^1J_{C-F}$ = 249.2 Hz, C_6F_5), 136.94 (d, $^1J_{C-F}$ = 237.7 Hz, C_6F_5), 133.44, 133.30, 128.47, 128.11, 127.80, 127.54, 126.72, 126.10, 124.65, 124.36, 123.99, 123.63, 123.26, 121.62, 118.56, 117.62, 104.41, 103.85 (18 resonances for indenyl-ring carbons), 102.05 (=*C*Me$_2$), 78.62 (α-*C*H$_2$, THF), 42.29 (N*Me*$_2$), 31.11 (*C*H$_2$CH$_2$), 30.32 (CH$_2$*C*H$_2$), 26.63 (β-*C*H$_2$, THF), 19.41 (=C*Me*$_2$), 17.45 (=C*Me*$_2$), 10.11 (B*C*H$_3$).

Isolation of *rac*-(EBI)Zr^+[OC(NH^{i}Pr)=CHCH$_2$C(Me$_2$)C(O^{i}Pr)=O][MeB($C_6F_5)_3$]$^-$ (4): The Single IPAA Addition Product of 1. In an argon-filled glovebox, a 30 mL glass reactor was charged with 49.2 mg (0.100 mmol) of *rac*-(EBI)ZrMe[OC(O^{i}Pr)=CMe_2], 58.4 mg (0.100 mmol) of ($C_6F_5)_3$B·THF, and 10 mL of CH_2Cl_2; this solution was allowed to stir for 10 min at ambient temperature, cleanly generating **1** in situ.[20] To this vigorously stirred solution of **1** in CH_2Cl_2 was added 11.3 mg (0.100 mmol) of IPAA at ambient temperature.

The color of the resulting mixture changed instantaneously from dark orange to bright yellow. The solution was stirred for 1 h, after which the volatiles were removed in vacuo to afford a sticky yellow solid. This crude product was washed with 3 × 2 mL hexanes and dried in vacuo to give 0.103 g (86%) of the pure title complex as a yellow powder. Anal. Calcd for $C_{52}H_{43}BF_{15}NO_3Zr$: C, 55.92; H, 3.88; N, 1.25. Found: C, 56.02; H, 4.19; N, 1.20.

^{1}H NMR (CD_2Cl_2, 23 °C) for **4** (generated in situ): δ 8.08 (d, J = 8.4 Hz, 1H), 7.81 (d, J = 8.4 Hz, 1H), 7.36−7.02 (m, 6H), 5.88 (d, J = 3.0 Hz, 1H), 5.79 (d, J = 3.0 Hz, 1H), 5.60 (d, J = 3.0 Hz, 1H), 5.46 (d, J = 3.0 Hz, 1H), 4.85 (d, J = 8.1 Hz, 1H, =C*H*), 4.65 (sept, J = 6.3 Hz, 1H, OC*H*Me$_2$), 4.30−3.96 (m, 2H, CH_2CH$_2$), 3.87−3.74 (m, 2H, CH$_2$CH_2), 3.68 (t, br, 4H, α-CH_2, free THF derived from **1**), 3.59 (sept, J = 6.6 Hz, 1H, HNC*H*Me$_2$), 1.97 (d, J = 13.8 Hz, 1H, CH_2), 1.82 (t, 4H, β-CH_2, free THF), 1.75 (d, J = 13.8 Hz, 1H, CH_2), 1.37 (d, J = 6.0 Hz, 3H, NCH*Me*$_2$), 1.22 (s, 3H, C*Me*$_2$), 1.20 (d, J = 6.0 Hz, 3H, OCH*Me*$_2$), 1.19 (d, J = 6.0 Hz, 3H, OCH*Me*$_2$), 1.14 (s, 3H, C*Me*$_2$), 1.05 (d, J = 6.0 Hz, 3H NCH*Me*$_2$), 0.49 (s, br, 3H, B*Me*). ^{19}F NMR (CD_2Cl_2, 23 °C): δ −131.45 (d, $^3J_{F-F}$ = 19.8 Hz, 6F, *o*-F), −163.58 (t, $^3J_{F-F}$ = 19.5 Hz, 3F, *p*-F), −166.14 (m, 6F, *m*-F). ^{13}C NMR (CD_2Cl_2, 23 °C): δ 185.59 [*C*(O^{i}Pr)=O], 171.40 [O*C*(NHMe$_2$)=], 148.77 (d, $^1J_{C-F}$ = 229.0 Hz, C_6F_5), 138.00 (d, $^1J_{C-F}$ = 234.5 Hz, C_6F_5), 136.90 (d, $^1J_{C-F}$ = 238.1 Hz, C_6F_5), 133.10, 130.60, 128.62, 128.36, 127.91, 127.51, 125.43, 124.57, 122.66, 122.52, 121.82, 121.39, 120.20, 119.44, 113.61, and 99.86 (indenyl carbons), 97.38 (−*C*H), 73.76 (α-*C*H$_2$, free THF), 68.35 (O*C*HMe$_2$), 43.47 (HN*C*HMe$_2$), 42.54 (*C*H$_2$), 39.54 (*C*Me$_2$), 31.82 (C*Me*$_2$), 30.91 (β-*C*H$_2$, free THF), 27.25 (C*Me*$_2$), 26.35 (*C*H$_2$CH$_2$), 26.12 (CH$_2$*C*H$_2$), 23.79, 22.51, 21.82, 20.93 (HNCH-*Me*$_2$, OCH*Me*$_2$), 10.80 (B*Me*).

Isolation of *rac*-(EBI)Zr$^+$[OC(NMe$_2$)=C(Me)CH$_2$C-(Me$_2$)C(NMe$_2$)=O][MeB(C$_6$F$_5$)$_3$]$^-$ (5): The Single DMMA Addition Product of 3. In an argon-filled glovebox, a 30 mL glass reactor was charged with 28.5 mg (0.060 mmol) of **2**, 35.0 mg (0.060 mmol) of $(C_6F_5)_3B$·THF, and 5 mL of CH_2Cl_2; this solution was allowed to stir for 10 min at ambient temperature, cleanly generating **3** in situ (vide supra). To this vigorously stirred solution of **3** in CH_2Cl_2 was added 7.3 μL (0.060 mmol) of DMMA at ambient temperature. The color of the resulting mixture changed instantaneously from dark red to light orange. The solution was stirred for 30 min, after which the volatiles were removed in vacuo to afford a sticky yellow solid. This crude product was washed with 5 × 2 mL hexanes and dried in vacuo to give 62.8 mg (95%) of the title complex as an orange powder.

^{1}H NMR (CD_2Cl_2, 23 °C) for **5**: δ 7.93 (d, J = 8.4 Hz, 1H), 7.75 (d, J = 8.4 Hz, 1H), 7.30−7.00 (m, 6H), 5.99 (d, J = 2.8 Hz, 1H), 5.71 (m, 2H), 5.56 (d, J = 2.8 Hz, 1H), 3.88−3.62 (m, 4H, CH_2CH_2), 3.23, 2.65, and 2.62 (s, 12H, N*Me*$_2$), 2.01 (d, J = 16.8 Hz, 1H, CH_2), 1.85 (d, J = 16.8 Hz, 1H, CH_2), 1.47 (s, 3H, =C*Me*), 1.39 (s, 3H, C*Me*$_2$), 1.38 (s, 3H, C*Me*$_2$), 0.50 (s, br, 3H, B*Me*). ^{19}F NMR (CD_2Cl_2, 23 °C): δ −131.42 (d, $^3J_{F-F}$ = 19.2 Hz, 6F, *o*-F), −163.48 (t, $^3J_{F-F}$ = 20.3 Hz, 3F, *p*-F), −166.07 (m, 6F, *m*-F). ^{13}C NMR (CD_2Cl_2, 23 °C): δ 180.56 [*C*(NMe$_2$)=O], 168.85 [O*C*(NMe$_2$)=], 148.90 (d, $^1J_{C-F}$ = 237.1 Hz, C_6F_5), 138.01 (d, $^1J_{C-F}$ = 243.0 Hz, C_6F_5), 136.97 (d, $^1J_{C-F}$ = 248.0 Hz, C_6F_5), 132.18, 130.37, 127.41, 126.80, 126.62, 126.27, 123.29, 122.88, 122.69, 122.50, 122.07, 115.83, 112.55, 103.40 (indenyl carbons), 101.56 (=*C*Me), 47.36 [C(N*Me*$_2$)=O], 41.35 (*C*H$_2$), 41.11 and 40.65 [OC(N*Me*$_2$)=], 38.14 (*C*Me$_2$), 30.36 (C*Me*$_2$), 29.27 and 28.98 (*C*H$_2$*C*H$_2$), 28.49 (C*Me*$_2$), 22.11 (=C*Me*), 10.80 (B*Me*).

X-ray Crystallographic Analysis of 2. Single crystals suitable for X-ray diffraction studies were grown by recrystallization from hexanes at −30 °C inside a freezer of the glovebox for 3 days and then quickly covered with a layer of Paratone-N oil (Exxon, dried and degassed at 120 °C/10^{-6} Torr for 24 h) after decanting the mother liquor. A crystal was then mounted on a thin glass fiber and transferred into the cold nitrogen steam of a Bruker SMART CCD diffractometer. Crystals of **2** were twinned by 180° rotation about the a axis. Identification of the twin law and deconvolution of the twinned diffraction patterns were accomplished by means of the Bruker software.[21a] The structure was solved by direct methods and refined by using the Bruker SHELXTL program library.[21b] The structure was refined by full-matrix least-squares on F^2 for all reflections, with two batch scale factors included to allow refinement against the deconvoluted data from the twinned crystal. All non-hydrogen atoms were refined with anisotropic displacement parameters, whereas hydrogen atoms were included in the structure factor calculations at idealized positions. The asymmetric unit of **2** contained two discrete molecules with similar structures. Selected crystallographic data for **2**: $C_{27}H_{31}NOZr$, monoclinic, space group $P2_1/c$, a = 16.3387(9) Å, b = 7.5650(4) Å, c = 36.764(2) Å, β = 94.242(1)°, V = 4531.7(4) Å^3, Z = 8, D_{calcd} = 1.398 mg/m^3, GOF = 1.104, $R1$ = 0.0523 [$I > 2\sigma(I)$], $wR2$ = 0.1052 (all data).

General Polymerization Procedures. Polymerizations were performed either in 30 mL, oven-dried glass reactors inside the glovebox or in 25 mL oven- and flame-dried Schlenk flasks interfaced to a dual-manifold Schlenk line. In a typical procedure, for polymerizations using the in situ generated **1**, a 2.5 mL stock solution of *rac*-(EBI)ZrMe[OC(O^{i}Pr)=CMe$_2$] (24.3 μmol) in CH_2Cl_2 was mixed in a flask with a solution of $(C_6F_5)_3B$·THF (24.3 μmol) in 2.5 mL of CH_2Cl_2 and stirred for 10 min to cleanly generate the cationic zirconocenium ester enolate **1**. DMAA (1.00 mL, 9.70 mmol) was quickly added via pipet (for polymerizations in the glovebox) or gastight syringe (for polymerizations on the Schlenk line), and the sealed flask was kept with vigorous stirring at the preequilibrated bath temperature. For polymerizations using the isolated active species **3**, 24.3 μmol of **3** was dissolved in 5 mL of CH_2Cl_2 in a 25 mL Schlenk flask. DMAA (1.00 mL, 9.70 mmol) was quickly added via gastight syringe, and the sealed flask was kept with vigorous stirring at the preequilibrated bath temperature. After the measured time interval, polymerizations were quenched by the addition of 5 mL of 5% HCl-acidified methanol. The quenched mixture was precipitated into 100 mL of diethyl ether and stirred for 30 min, and the solvent was decanted off. An additional 75 mL of diethyl ether was used to wash the polymer and then decanted. The P(DMAA) product was obtained as a sticky solid and dried in a vacuum oven at 50 °C overnight to a constant weight. The polymer was dissolved in minimum CH_2Cl_2 or MeOH, precipitated into a 10-fold excess of diethyl ether, stirred for 30 min, filtered, washed with diethyl ether, and dried in a vacuum oven at 50 °C for 48 h to a constant weight. The P(DMAA) polymers obtained are white fibrous materials.

Polymerization Kinetics. The procedures already developed for the kinetic studies of methacrylate polymerization[20] were modified for the kinetic experiments of acrylamide polymerization. The experiments were carried out in stirred Schlenk flasks at 23 °C using the same polymerization procedure as already described above, except that, at appropriate time intervals, 0.2 mL aliquots were withdrawn from the reaction mixture via syringe and quickly quenched into 1 mL vials containing 0.6 mL of undried "wet" $CDCl_3$ stabilized by 250 ppm of BHT-H. The quenched aliquots were analyzed by ^{1}H NMR. The ratio of $[DMAA]_0$ to $[DMAA]_t$ at a given time t, $[DMAA]_0/[DMAA]_t$, was determined by integration of the peaks for DMAA (6.3−6.1 and 5.7−5.5 ppm for the vinyl proton signals) and P(DMAA) (centered at 2.5 ppm for the methine proton signal) according to $[DMAA]_0/[DMAA]_t = (\mathbf{A}_{2.5}/\mathbf{A}_{5.6+6.2}) + 1$, where $\mathbf{A}_{2.5}$ is the total integrals for the peaks centered at 2.5 ppm (typically in the region 2.3−2.6 ppm) and $\mathbf{A}_{5.6+6.2}$ is the total integrals for the vinyl protons in the regions 5.7−5.5 and 6.3−6.1 ppm. Apparent rate constants (k_{app}) were extracted from the slopes of the best fit lines to the plots of $\ln([DMAA]_0/[DMAA]_t)$ vs time.

Polymer Characterizations. The low-molecular-weight P(DMAA) sample was analyzed by matrix-assisted laser desorption/ionization time-of-flight mass spectroscopy (MALDI-TOF MS); the experiment was performed on an Ultraflex MALDI-TOF mass spectrometer (Bruker Daltonics) operated in reflector mode using a Nd:YAG laser at 355 nm and 25 kV accelerating voltage. A thin layer of a 1% NaI solution was first deposited on the target plate, followed by 1 μL of both sample and matrix (dithranol, 10 mg/mL in MeOH).

Chart 1. Polymerization of DMAA by 1, Producing P(DMAA) (Left) with [*mm*] >99% (Middle: ^{13}C NMR Spectrum in D_2O at 80 °C), and PDI = 1.07 (Right: GPC Trace)

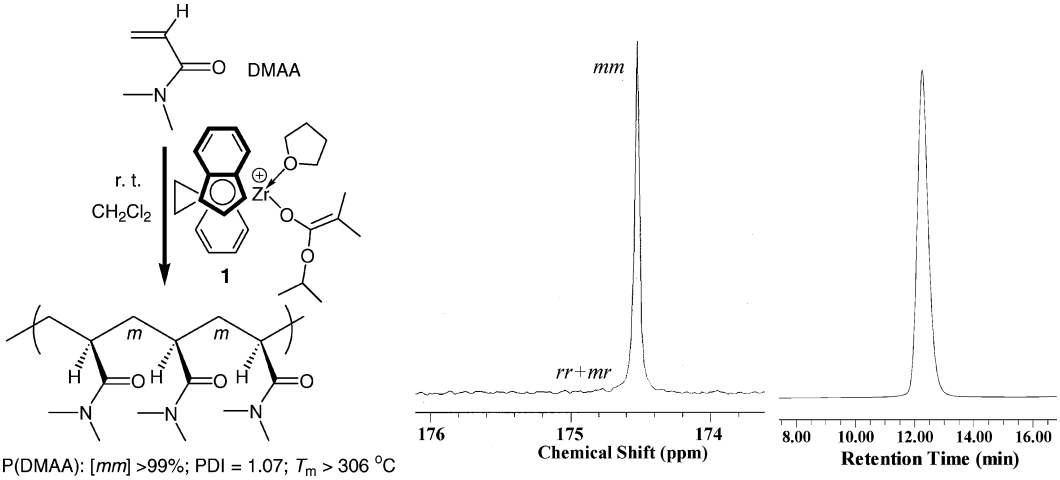

Methods and procedures for characterizations of the polymer glass transition temperature (T_g) and melting transition temperature (T_m), maximum rate decomposition temperature (T_{max}), number-average molecular weight (M_n), and molecular weight distribution (M_w/M_n) as well as microstructures (^{1}H NMR *m*/*r* dyads and ^{13}C *mm*/*rr*+*mr* triads) were previously described.[7,20]

Results and Discussion

The first stereospecific coordination polymerization of DMAA was effected by the chiral *ansa*-zirconocenium ester enolate **1**, which produces P(DMAA) with unprecedented isotacticity ([*mm*]) of >99%, high M_n of ~10^5 g/mol, low polydispersity index (PDI = M_w/M_n) of 1.07, T_m of >306 °C, and T_{max} of >420 °C (Chart 1).[7] However, mechanistic details about the DMAA polymerization by chiral *ansa*-zirconocenium enolates and the scope of this polymerization for other acrylamides were unknown and, thus, became the focus of the present study.

Kinetics of DMAA Polymerization by 1. The chiral *ansa*-zirconocenium ester enolate **1** can be either isolated[9a] or cleanly generated in situ by mixing of the neutral methyl zirconocene ester enolate precursor, *rac*-(EBI)ZrMe[OC(O^{i}Pr)=CMe$_2$], with $(C_6F_5)_3B$·THF in CH_2Cl_2 at room temperature.[20] The cation **1** is stable in a solution of CH_2Cl_2 at room temperature; subsequently, the in situ generated **1** in CH_2Cl_2 was used for the DMAA polymerization and kinetic studies.

Typical results of DMAA polymerization by **1** in CH_2Cl_2 at 23 °C are summarized in Table 1. As shown in Table 1, the polymerization of DMAA by **1** with $[DMAA]_0/[\mathbf{1}]_0$ ratios = 400−1500 is rapid and efficient with initiator efficiencies (I^*) ranging from moderate 70% to high 93% and produces P(DMAA) with low PDI values ranging from 1.04 to 1.24. All P(DMAA) produced are highly isotactic ([*mm*] > 99%). Several lines of evidence, including the aforementioned polymerization characteristics, the production of the well-defined diblock copolymer P(MMA)-*b*-P(DMAA) with a small PDI value of 1.07 (vide infra), and the observed linear increase of the polymer M_n with $[DMAA]_0/[\mathbf{1}]_0$ ratios and with monomer conversion, which is coupled with the small, nearly constant PDI values (Figure 1), clearly demonstrate living characteristics of this polymerization.

Results of the polymerization kinetic studies using complex **1** at 23 °C in CH_2Cl_2 with a broad range of $[DMAA]_0/[\mathbf{1}]_0$ ratios from 400 to 1500 clearly show that propagation is first order in [DMAA] for all the $[DMAA]_0/[\mathbf{1}]_0$ ratios investigated in this study (Figure 2). A double-logarithm plot (Figure 3) of the apparent rate

Table 1. Selected DMAA Polymerization Results by Chiral *ansa*-Zirconocenium Ester Enolate Complex 1 in CH_2Cl_2 at 23 °C[a]

run no.	[**1**] (mmol/L)	$[DMAA]_0/[\mathbf{1}]_0$	time (min)	conv (%)	$10^4 M_n$[b] (g/mol)	PDI[b] (M_w/M_n)	I^*[c] (%)
1	4.85	400	1	16	0.75	1.06	0.85
2			2	28	1.47	1.05	0.75
3			3	37	2.05	1.05	0.71
4			8	69	3.61	1.06	0.76
5			12	80	4.07	1.08	0.78
6			15	88	4.21	1.09	0.83
7			25	96	4.53	1.10	0.84
8	3.23	600	1	10	0.61	1.09	0.93
9			2	18	1.27	1.06	0.86
10			3	25	1.87	1.05	0.79
11			8	52	4.03	1.05	0.76
12			12	65	4.87	1.06	0.79
13			15	72	5.32	1.07	0.80
14			20	80	5.30	1.11	0.89
15			25	88	5.88	1.10	0.89
16			45	98	6.42	1.12	0.90
17	1.94	1000	2	9	1.13	1.08	0.80
18			3	13	1.78	1.07	0.73
19			5	28	2.98	1.06	0.91
20			14	46	6.25	1.07	0.74
21			20	56	7.25	1.11	0.77
22			30	78	10.30	1.09	0.75
23			40	84	10.24	1.13	0.81
24			60	95	13.03	1.11	0.72
25	1.62	1200	5	21	3.52	1.05	0.70
26			14	46	7.90	1.06	0.70
27			20	55	8.87	1.10	0.74
28			40	81	11.41	1.20	0.84
29			60	90	13.31	1.21	0.80
30			70	91	13.35	1.23	0.81
31			90	92	13.77	1.22	0.80
32	1.29	1500	2	8	1.26	1.06	0.90
33			5	17	3.12	1.05	0.80
34			8	23	4.79	1.04	0.70
35			14	37	7.29	1.05	0.74
36			20	45	8.83	1.07	0.76
37			30	58	10.46	1.11	0.83
38			40	68	11.61	1.16	0.87
39			50	75	13.48	1.17	0.82
40			100	90	15.85	1.24	0.84

[a] All polymerizations were carried out in flame-dried Schlenk flasks on a Schlenk line using an external temperature-control bath set at 23 °C. [b] M_n and PDI determined by GPC relative to PMMA standards in $CHCl_3$. [c] Initiator efficiency (I^*) = M_n(calcd)/M_n(exptl), where M_n(calcd) = MW(DMAA) × $[DMAA]_0/[\mathbf{1}]_0$ × conversion.

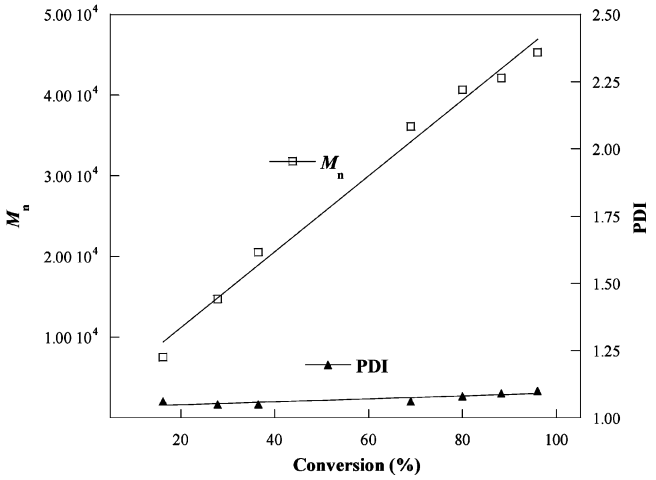

Figure 1. Plot of M_n and PDI of PDMAA by **1** {$[DMAA]_0/[\mathbf{1}]_0$ = 400; 23 °C} vs monomer conversion.

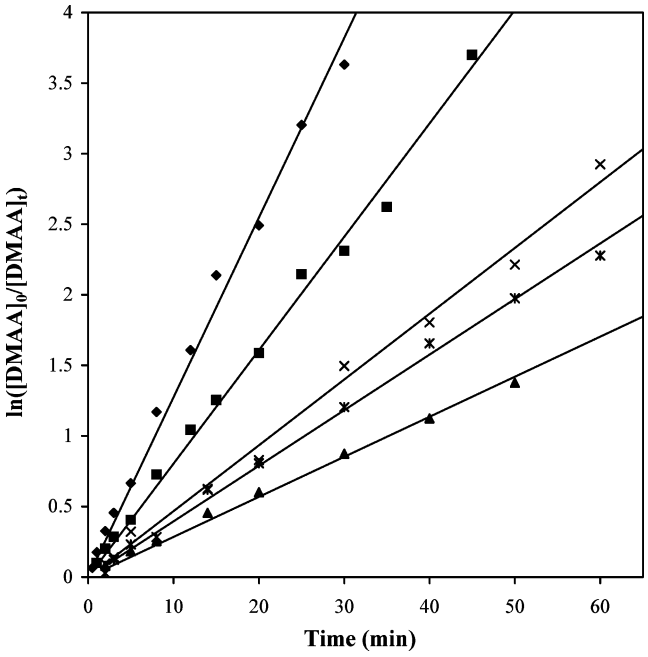

Figure 2. Semilogarithmic plots of $\ln\{[DMAA]_0/[DMAA]_t\}$ vs time for the polymerization of DMAA by **1** in CH_2Cl_2 at 23 °C. Conditions: $[DMAA]_0$ = 1.94 M; $[\mathbf{1}]_0$ = 4.85 (◆), 3.23 (■), 1.94 (×), 1.62 (∗), and 1.29 mM (▲).

constants (k_{app}), obtained from the slopes of the best-fit lines to the plots of $\ln([DMAA]_0/[DMAA]_t)$ vs time, as a function of ln[**1**] was fit to a straight line (R^2 = 0.998) of slope = 1.1(1). The kinetic order with respect to [**1**], given by the slope of 1.1(1), reveals that propagation is also first order in [Zr], indicating a *monometallic*, intramolecular coordinative-conjugate-addition propagation mechanism.

Polymer Chain-End Groups. To identify the initiation and termination chain-end groups and further confirm the living nature of this polymerization, the low-molecular-weight P(DMAA) produced by **1** in a $[DMAA]_0/[\mathbf{1}]_0$ ratio of 20:1 was characterized by MALDI-TOF mass spectrometry (Figure 4). The plot of *m/z* values in the MALDI-TOF mass spectrum vs the number of DMAA repeat units (n) yielded a straight line with a slope of 99.07 and an intercept of 152.86 (Figure 5); the slope corresponds to the mass of the DMAA monomer, whereas the intercept is the sum of the masses of Na^+ (from the added NaI) and the chain-end groups which

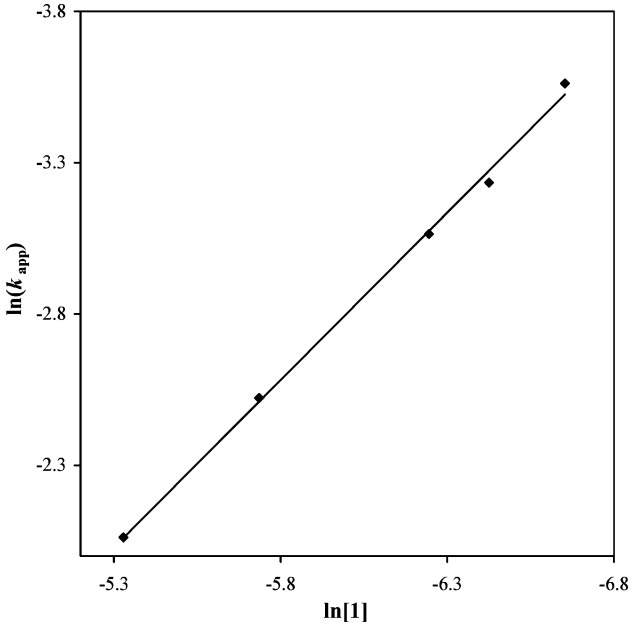

Figure 3. Plot of $\ln(k_{app})$ vs ln[**1**] for the DMAA polymerization by **1** in CH_2Cl_2 at 23 °C.

correspond to a formula of $C_7H_{14}O_2$. This analysis clearly shows that the polymer has a structural formula of ^{i}PrOC(=O)C(Me_2)−(DMAA)$_n$−H, where the initiation chain end [^{i}PrOC(=O)C(Me_2)−] is derived from the initiating isopropyl isobutyrate group in complex **1** and the termination chain end (H) from the HCl-acidified methanol during the workup procedure.

Block Copolymerization of MMA and DMAA. Sequential block copolymerization of MMA and DMAA by **1** in CH_2Cl_2 at 23 °C with $[MMA]_0/[DMAA]_0/[\mathbf{1}]_0$ = 400/400/1, starting from polymerization of MMA followed by polymerization of DMAA, afforded the well-defined diblock copolymer P(MMA)-*b*-P(DMAA) (Figure 6). The block copolymer has an M_n of 1.33 × 10^5 g/mol and a PDI value of 1.07. The molar composition of the two monomer units in the block copolymer obtained from the ^{1}H NMR analysis is the same as the monomer molar feed ratio (i.e., 1:1). Both blocks are highly isotactic, with isotacticity of [*mm*] = 93% for the P(MMA) block and of [*mm*] > 99% for the P(DMAA) block. As can be seen in Figure 6, this block copolymer exhibits a T_g characteristic of the isotactic P(MMA) component segment (T_g = 63 °C) and a T_m characteristic of the isotactic P(DMAA) component segment (T_m = 313 °C). Owing to the high crystallinity of the highly isotactic P(DMAA) block, there is no apparent T_g, but a distinct T_m, for this component segment; this is the same as what has been observed for the highly isotactic homopolymer P(DMAA).[7]

Polymerization Mechanism. In sharp contrast to the facile formation of the previously mentioned diblock copolymer P(MMA)-*b*-P(DMAA), the sequential block copolymerization starting from polymerization of DMAA followed by polymerization of MMA, or the statistical copolymerization using a 1:1 DMAA:MMA monomer pool, afforded only homopolymer P(DMAA)! The results of the DMAA homopolymerization by **1** showed living characteristics (vide supra); to further confirm the living nature of the active propagating species derived from the DMAA polymerization, a reinitiation experiment was carried out (**1** to **A** to **B** to **C**, Scheme 1). Note that structures **A**, **B**, and **C** were modeled by isolated

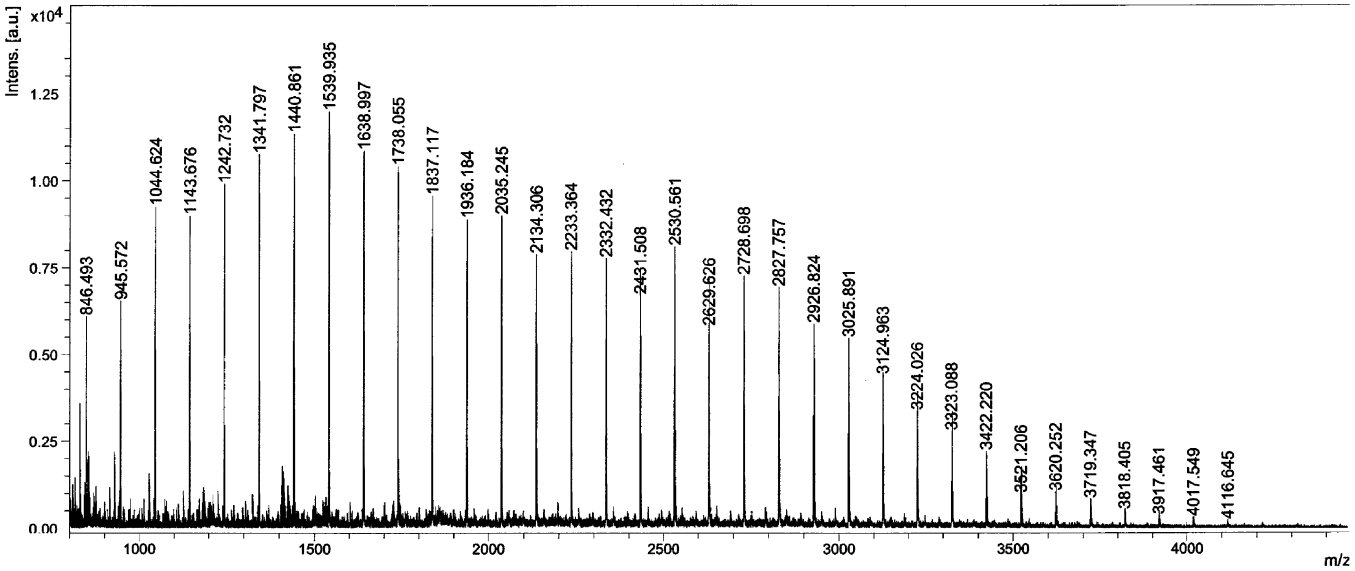

Figure 4. MALDI-TOF mass spectrum of the low-molecular-weight P(DMAA) produced by **1** in CH_2Cl_2 at 23 °C with $[DMAA]_0/[\mathbf{1}]_0 = 20:1$; the sample analyzed was as quenched and unpurified.

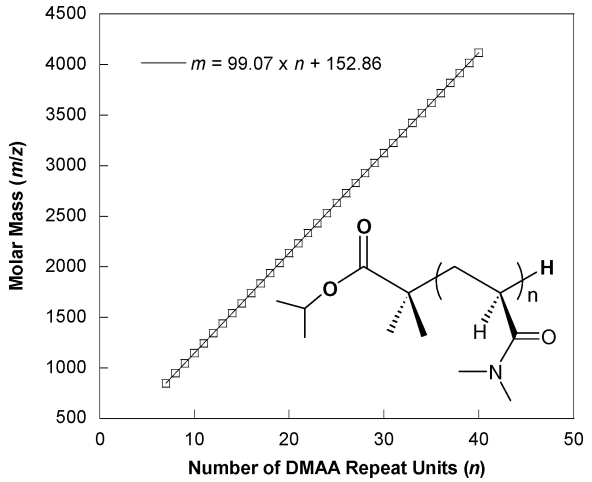

Figure 5. Plot of *m/z* values from Figure 4 vs the number of DMAA repeat units (*n*).

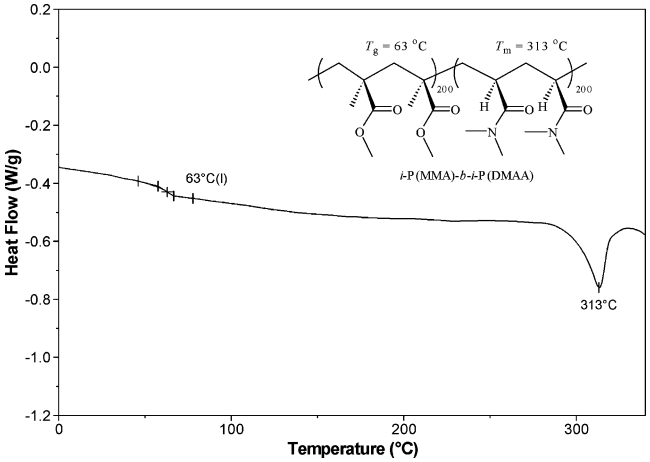

Figure 6. DSC trace of diblock copolymer P(MMA)-*b*-P(DMAA) produced by **1** in CH_2Cl_2 at 23 °C.

complexes (vide infra) and that the DMAA propagation cycle (**B** ↔ **C**) is the same as that proposed for the MMA polymerization,[20] on the basis of the kinetic results. Thus, after the first portion of DMAA was completely consumed by **1**, a 45 min delay was implemented before addition of a second portion of DMAA. This polymerization sequence yielded highly isotactic P(DMAA)-*b*-P(DMAA) in quantitative yield with an M_n greater than double that of the individual block and a low PDI of 1.07, further confirming the living nature of the active propagating species **B**. On the basis of these results, the inability of the living propagating species derived from the DMAA polymerization by **1** to further polymerize MMA can be attributed to either of the following two scenarios: (a) MMA is unable to enter the preoccupied coordination site of the cationic Zr center due to stronger binding of the amide oxygen of the penultimate DMAA unit to Zr than the ester oxygen of MMA to Zr (i.e., step (iii), **C** → **D**, is not feasible), and subsequently MMA cannot be activated for the polymerization to proceed; or (b) MMA is able to displace the coordinated penultimate amide group and thus enter the coordination site of the cationic Zr center, but the polymeric amide enolate ligand derived from DMAA polymerization is not active enough to undergo nucleophilic addition to the activated MMA (i.e., step (iv), **D** → **E**, is not feasible).

To test these hypotheses, it became necessary to independently synthesize the chiral *ansa*-zirconocene amide enolate *rac*-(EBI)ZrMe[OC(NMe$_2$)=CMe$_2$] (**2**) and the corresponding cationic complex *rac*-(EBI)Zr$^+$(THF)-[OC(NMe$_2$)=CMe$_2$][MeB(C$_6$F$_5$)$_3$]$^-$ (**3**). Intuitively, the amide enolate moiety in structure **D** should be more nucleophilic than the ester enolate moiety in **1**, and thus, step (iv) is unlikely the reason for the inability of the living propagating species **B** to further polymerize MMA; however, ruling out this possibility requires an independent study of the MMA polymerization behavior using the isolated cationic amide enolate **3**. Furthermore, complex **3** models the structure of the proposed active propagating species **B** (Scheme 1). Therefore, polymerization studies using complex **3** will offer unique opportunities for a better understanding of the polymerization of acrylamides and copolymerization of acrylamides with MMA by metallocene complexes.

Scheme 2 outlines the reaction sequences leading to **2** and **3** through the *ansa*-zirconocene methyl triflate intermediate *rac*-(EBI)ZrMe(OTf),[9a] which was synthesized utilizing the comproportionation reaction between *rac*-(EBI)ZrMe$_2$ and *rac*-(EBI)Zr(OTf)$_2$, the latter of

Scheme 1

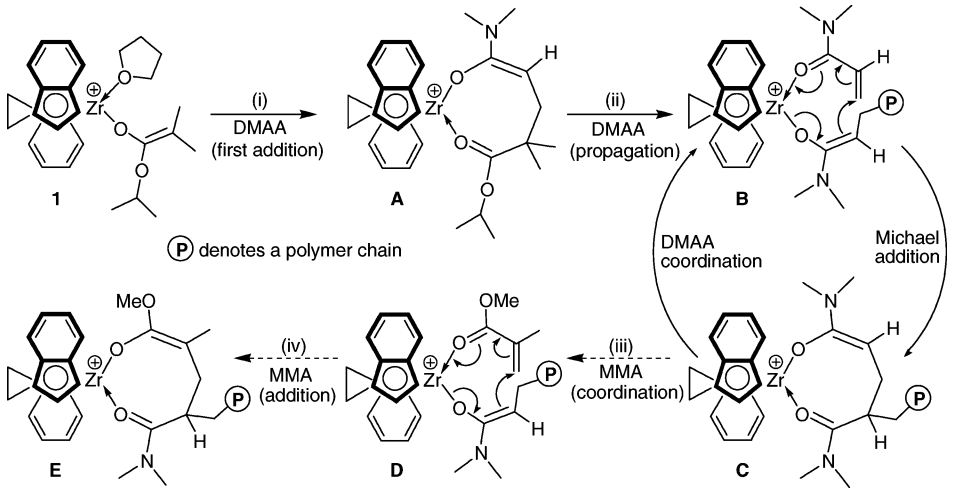

Scheme 2

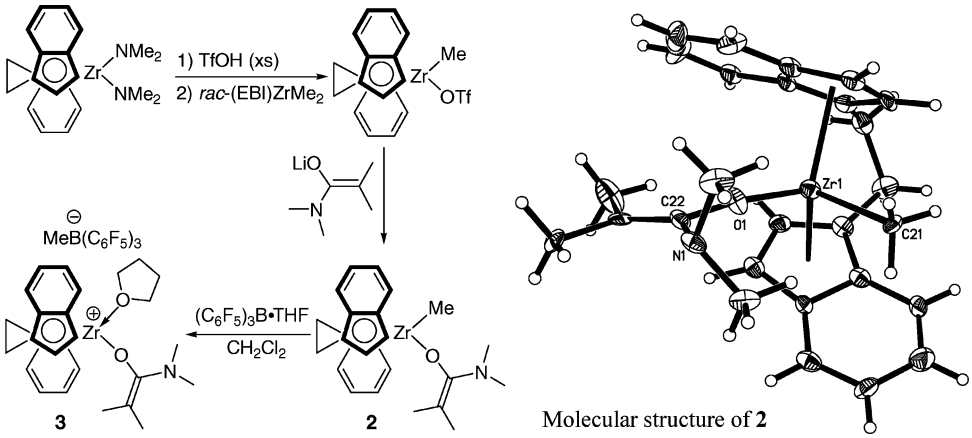

which was prepared from the reaction *rac*-(EBI)Zr-$(NMe_2)_2$ with excess triflic acid (TfOH). The subsequent reaction of *rac*-(EBI)ZrMe(OTf) with lithium amide enolate $LiOC(NMe_2)=CMe_2$ in toluene proceeds cleanly to produce the chiral zirconocene amide enolate **2** in 96% isolated yield. The ^{1}H NMR spectrum shows C_1 symmetry for **2** in solution, featuring four nonequivalent protons for the C_5 rings of the bis(indenyl) ligand (Figure 7, bottom), whereas the X-ray crystal structure of **2** reveals a unique *s-trans* conformation as to the Zr−Me and C=C bonds about the nearly linear Zr−O−C vector (Scheme 2). We have previously shown that metallocene *ester* enolates adopt a *s-cis* conformation;[9a,13a] the observed *s-trans* conformation in the solid-state structure of the *amide* enolate **2** is presumably a result of placing the bulky NMe_2 group into the coordination sphere voids of the *rac*-structure by minimizing the steric interactions of the NMe_2 group with the indenyl phenyl ring. Adopting such an *s-trans* conformation for the zirconocenium amide enolate impacts its polymerization behavior (vide infra).

Erker and co-workers showed that the reaction of zirconocene *ketone* enolates with $B(C_6F_5)_3$ forms direct adducts via borane addition to the nucleophilic enolate carbon center.[22] However, the NMR-scale reaction of the methyl zirconocene *N,N*-dimethylisobutyramide enolate **2** with $(C_6F_5)_3B$•THF in CD_2Cl_2 at ambient temperature cleanly produces the methide-abstraction product—the cationic zirconocenium amide enolate **3** (Figure 7, top). This conclusion is established chiefly by the observation of the disappearance of the Zr*Me* signal (−0.53 ppm) in **2** and the appearance of a characteristic, broad singlet at 0.51 ppm for the B*Me* in **3**; this chemical shift for the methyl group in the $[MeB(C_6F_5)_3]^-$ anion in CD_2Cl_2 is identical to that reported in the literature for the free $[MeB(C_6F_5)_3]^-$ anion.[23] The noncoordinating nature of the $[MeB(C_6F_5)_3]^-$ anion in **3** is also established by the ^{19}F NMR spectrum in which a small chemical shift difference of <3 ppm [$\Delta(m,p\text{-F}) = 2.6$ ppm in **3**] between the *para*- and *meta*-fluorines is diagnostic of the noncoordinating $[MeB(C_6F_5)_3]^-$ anion.[23,24] The preparative scale reaction in CH_2Cl_2 at ambient temperature gave the analytically pure cationic zirconocenium amide enolate **3** in 96% isolated yield. The selectivity of the methide abstraction over the possible borane addition in the reaction of **2** with the borane seems to be sterically directed; the reaction of the analogous but less bulky methyl zirconocene *N,N*-dimethylpropanamide enolate with $(C_6F_5)_3B$•THF under identical conditions yielded a messy product mixture, presumably due to a scenario where both reaction modes (i.e., methide abstraction by the borane and borane addition to the C=C bond) are operative in this reaction.

Subsequently, we carried out polymerizations of DMAA and MMA using the isolated cation **3** in CH_2Cl_2 at 23 °C, the key results of which are summarized in Table 2. The polymerization of DMAA by **3** ($[DMAA]_0/[\mathbf{3}]_0 = 400/1$) proceeded in a manner similar to that of **1** and achieved a high monomer conversion of 96% in 30 min, producing highly isotactic P(DMAA) with a low PDI value and essentially a quantitative initiator efficiency (run 1, Table 2). It is interesting to note,

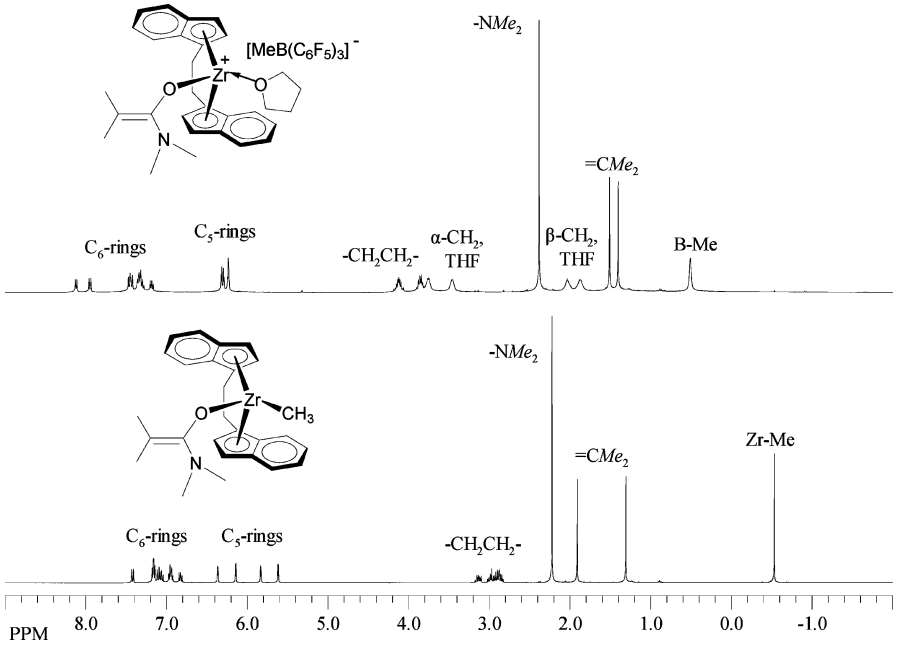

Figure 7. ^{1}H NMR spectra (23 °C) of **2** (C_6D_6, bottom) and **3** (CD_2Cl_2, top).

Table 2. DMAA and MMA Polymerization Results by Chiral *ansa*-Zirconocenium Amide Enolate Complex 3[a]

run no.	monomer	[**3**] (mmol/L)	$[monomer]_0/[\mathbf{3}]_0$	time (min)	conv (%)	$10^4 M_n$ (g/mol)	PDI (M_w/M_n)	I^* (%)
1	DMAA	4.85	400	30	96	3.58	1.12	1.06
2	MMA	4.85	400	120	~0			

[a] See Table 1 footnotes for explanations of parameters listed in the table.

however, a subtle difference in the DMAA polymerization behavior between **1** and **3**: unlike the *ester* enolate **1**, which does not exhibit any induction (initiation) period (see Table 1 or Figure 2), the *amide* enolate **3** shows a ca. 5 min induction period, after which the kinetic profile is similar to that of **1**. This observed difference between **1** and **3** can be directly related to the difference in their preferred conformations—the *s-cis* conformation (as to the Zr←monomer and C=C bonds about the Zr−O−C vector) for the ester enolate vs the *s-trans* conformation for the amide enolate (vide supra), assuming that the cations (where the Zr←monomer bond displaces the Zr−Me bond in the neutral species) adopt the same more stable conformation as the corresponding neutral precursors. In this context, a conversion from the preferred *s-trans* amide enolate conformation to the *s-cis* amide enolate conformation shown in **B** (Scheme 1) is required before the intramolecular Michael addition can take place, accounting for the observed induction period of the amide enolate **3**. After this induction period, the needed *s-cis* amide enolate conformation ready for the facile C−C formation step is preserved throughout the polymerization reaction because the Michael addition is faster than the rate-limiting monomer coordination step in the proposed "catalytic" propagation cycle (Scheme 1).

As anticipated, the MMA polymerization using **3** in CH_2Cl_2 afforded no polymeric products over a 2 h period; however, monitoring the equimolar reaction of **3** and MMA via ^{1}H NMR (CD_2Cl_2, 23 °C) clearly shows the disappearance of the MMA vinyl signals and the appearance of a new set of resonances consistent with the formation of the single-MMA-addition product,[20] *rac*-(EBI)Zr^+[OC(OMe)=C(Me)CH_2C(Me_2)C(NMe_2)=O][$MeB(C_6F_5)_3$]$^-$ (i.e., structure **E**, Scheme 1). These results indicate that the observed copolymerization behavior can be attributed to the inability of MMA to displace the coordinated, more basic amide oxygen of the cyclic amide enolate intermediate **C** (i.e., step (iii) is not feasible); this is further supported by the competitive binding experiment which shows the ion pair *rac*-(EBI)$ZrMe^+MeB(C_6F_5)_3^-$ prefers to bind *N*-isopropylacrylamide over methyl isobutyrate in a 1:1:1 mixture.

Scope of Polymerization of Acrylamides. Polymerizations of *N*,*N*-dimethylmethacrylamide (DMMA) and *N*-isopropylacrylamide (IPAA) using both ester and amide enolates **1** and **3** were attempted, but neither complex yielded polymer products. The lack of polymerizability of DMMA has also been previously noted in anionic polymerizations by organolithium initiators, which was attributed to insufficient stabilization of the amide enolate intermediates as a result of nonbonding interactions between the α-methyl group or the vinyl proton and the *N*-methyl group;[3] such nonbonding interactions are believed to cause twisting of the carbonyl−vinyl C−C single bond, leading to a twisted monomer conformation for a less effective overlap of the vinyl carbonyl π bonds (i.e., conjugation between two π bonds) than usually found in the planar conformation.[25] The problems associated with the polymerization of IPAA by common anionic initiators seem more straightforward because of the presence of the acidic amide NH hydrogen in IPAA. Nevertheless, the observed same nonpolymerizability of DMMA or IPAA in coordination polymerization using chiral *ansa*-zirconocenium enolates could be due to the very same or a completely different reason. To seek for this answer, we set out to investigate stoichiometric reactions of **1** with IPAA and **3** with DMMA as well as subsequent reactions of their products with an excess of monomer.

We initially reasoned that the lack of activity of the IPAA polymerization by **1** was likely due to the presence

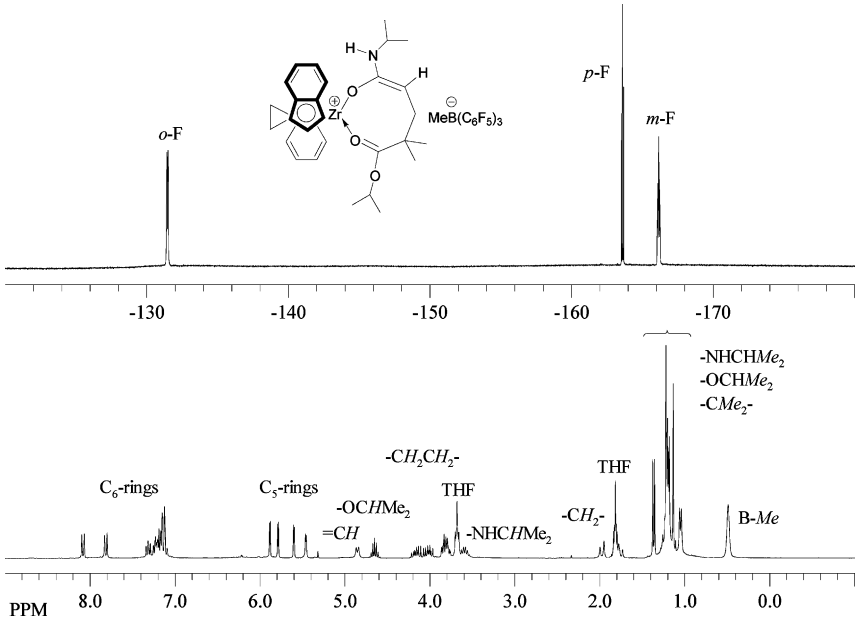

Figure 8. ^{1}H (bottom) and ^{19}F NMR spectra of **4** generated in situ by mixing of **1** and IPAA in CD_2Cl_2 at 23 °C (note the internal NMR solvent reference peak at 5.32 ppm).

Scheme 3

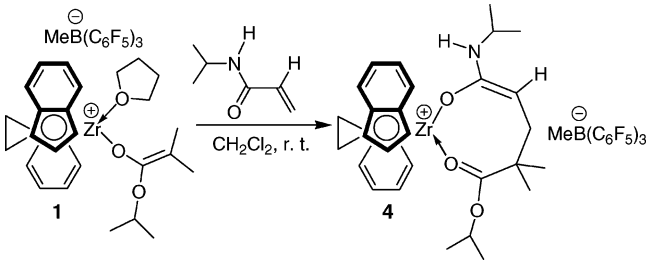

of the acidic amide NH hydrogen in IPAA. However, monitoring the reaction of **1** with 1 equiv of IPAA by ^{1}H and ^{19}F NMR in CD_2Cl_2 shows facile addition of IPAA to **1**, with no evidence for catalyst decomposition, but all evidence pointing to a *clean* formation of the single IPAA addition product, *rac*-(EBI)Zr^{+}[OC(NH-^{i}Pr)=CHCH$_2$C(Me$_2$)C(O^{i}Pr)=O][MeB(C$_6$F$_5$)$_3$]$^{-}$ (**4**) (Figure 8).

The single IPAA addition product **4** is stable in CD_2Cl_2 at ambient temperature, and no decomposition was detected over a period of 8 h at this temperature. Subsequently, a preparative scale reaction afforded **4** in 86% isolated yield (Scheme 3). (Note that in the preparative scale reaction the displaced THF can be removed during drying the product in vacuo.) In the presence of excess IPAA, no further IPAA additions took place after the first IPAA addition to **1**, even with an extended reaction time (24 h). Attempts to polymerize IPAA by mixing **1** with 400 equiv of IPAA in 1,2-dichlorobenzene at temperatures from 23 to 80 °C, or in bulk at 100 °C, afforded no polymer products. Likewise, polymerizations of IPAA by **3** under varied conditions also afforded no polymer products.

The proposed structure for **4** was based on the spectroscopic and analytical characterizations (see Figure 8 and Experimental Section), while attempts to obtain its crystal structure were unsuccessful. Nevertheless, both ^{1}H and ^{13}C NMR spectra of **4** feature characteristic signals for a zirconocenium amide enolate structure and additionally an isopropyl ester group [−C(O^{i}Pr)=O]. Specifically, the ^{1}H NMR signal for −OC*H*Me$_2$ (3.73 ppm) attached to the enolate ligand in **1**[9a] is substantially downfield shifted to 4.65 ppm (sept) for −OC*H*Me$_2$ now attached to the ester group in **4**; the ^{13}C NMR chemical shift difference confirms these assignments: 154.07 ppm for the enolate *C*(O) carbon [(O*C*(O^{i}Pr)=] in **1**[9a] vs 185.59 ppm for the ester *C*(O) carbon [*C*(O^{i}Pr)−O] in **4**. In agreement with these spectroscopic changes for the reaction of **1** + IPAA → **4**, the added IPAA becomes an isopropyl amide enolate ligand [i.e., −OC(NH^{i}Pr)=CHCH$_2$−] attached to Zr in **4**, which can be readily characterized by ^{1}H NMR [4.85 (−C*H*), 3.59 (HNC*H*Me$_2$), 1.97 and 1.75 (C*H*$_2$), 1.37 and 1.05 (HNCH*Me*$_2$)] and by ^{13}C NMR {171.40 [O*C*(NH^{i}-Pr)=], 97.38 (=*C*H), 43.47 (HN*C*HMe$_2$), 42.54 (*C*H$_2$)}.

The single IPAA addition product **4** does not effect further IPAA additions, but it rapidly polymerizes DMAA to highly isotactic P(DMAA), much like the cationic complexes **1** and **3**. Thus, the inability of **1**, **3**, or **4** to polymerize IPAA is likely due to sterics of IPAA vs DMAA, not because of the reactivity of the cyclic amide enolate **4**. The significance of isolating the cyclic zirconocenium amide enolate species **4** is that it corresponds to the structure of the eight-membered-ring propagating intermediates (i.e., structures **A** and **C**, Scheme 1) involved in the acrylamide polymerization, thereby providing further direct evidence supporting the proposed monometallic, coordination polymerization of acrylamides by zirconocenium enolates proposed in Scheme 1.

The reaction of **3** with DMMA was also investigated in the same manner as the reaction of **1** with IPAA. Significantly, the single DMMA addition product (**5**) was isolated in quantitative yield (Scheme 4; see Experimental Section for spectroscopic data). Upon addition of another equivalent DMMA, no further addition took place, and the added second equivalent DMAA remains as free monomer in solution. The reaction of **3** with IPAA follows a similar pattern. These results indicate that initiations via conjugate addition occur readily; however, propagation steps involving further monomer additions are problematic, primarily due to steric reasons that keep the incoming monomer from entering the

Scheme 4

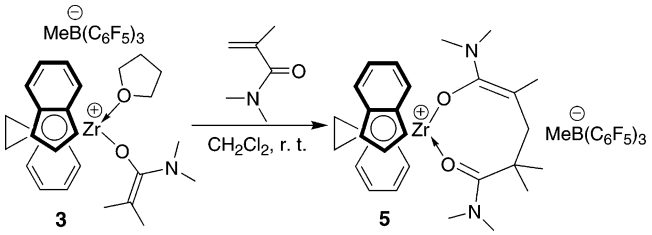

coordination site at the metal via ring opening of the chelate amide enolate intermediate.

Conclusions

We have investigated the mechanism and scope of the metallocene-mediated isospecific coordinative-anionic polymerization of acrylamides, using the chiral zirconocenium ester and amideenolates **1** and **3**. The ester enolate complex **1** effects the highly isospecific[26] and living polymerization of DMAA, producing P(DMAA) with remarkably high [*mm*], T_m, and T_{max} values. Kinetic studies of the DMAA polymerization by **1** have shown that propagation is first order in both concentrations of the monomer and the active species. These results, coupled with those from the studies of the isolation and characterization of several model complexes, demonstrate that this DMAA polymerization proceeds via a monometallic, coordinative-conjugate-addition mechanism through cyclic amide enolate intermediates (i.e., structure **C**, Scheme 1). The results imply that the resting state during a "catalytic" propagation cycle is the cyclic amide enolate **C** and associative displacement of the coordinated amide group by incoming acrylamide monomer to regenerate the active species **B** is the rate-determining step.

Success in the production of the well-defined isotactic diblock copolymers of methacrylates and acrylamides hinges on the comonomer addition sequence. Thus, sequential block copolymerization starting from polymerization of MMA by **1**, followed by polymerization of DMAA, produces isotactic diblock copolymer P(MMA)-*b*-P(DMAA). However, owing to the inability of MMA to enter the coordination site of Zr that is preoccupied by the amide group of the penultimate DMAA unit, only homopolymer P(DMAA) is produced when the monomer addition sequence is reversed.

To confirm the proposed active propagating structure for the polymerization of acrylamides, we have synthesized model zirconocene amide enolate complexes: neutral chiral amide enolate **2** and the corresponding cationic species **3**. Much like the ester enolate species **1**, except for the initiation behavior, the isolated amide enolate species **3** effects facile DMAA polymerization leading to highly isotactic and high-molecular-weight P(DMAA) with high initiator efficiency, thereby serving as a suitable structural model for the living active propagating species (i.e., structure **B**, Scheme 1).

Unlike DMAA, sterically hindered acrylamides such as DMMA and IPAA are not polymerized by either chiral zirconocenium ester enolate **1** or amide enolate **3**, primarily due to steric reasons incurred in the propagation step. However, initiation occurs readily, supported by the observation of the facile additions of 1 equiv of IPAA to **1** and 1 equiv of DMMA to **3**, generating the isolable eight-membered-ring cyclic amide enolates **4** and **5**, respectively; these cyclic amide enolates correspond to the structures of the first acrylamide addition product of **1** (i.e., structure **A**, Scheme 1) and the resting propagation intermediate (i.e., structure **C**, Scheme 1). An interesting question naturally emerged in light of these results is, can these monomers (DMMA and IPAA) be polymerized by more sterically open catalysts or by rendering polymerization reactions to proceed via different mechanisms? Research seeking for an answer to this question is currently underway.

Acknowledgment. This work was supported by the National Science Foundation and Colorado State University. The Bruker X-ray diffractometer was purchased with a grant from the NIH Shared Instrumentation Grant Program. We thank Prof. Oren P. Anderson (CSU), Ms. Susie M. Miller (CSU), and Dr. Charles Campana (Bruker AXS) for determination of the crystal structure as well as Boulder Scientific Co. for the gift of $B(C_6F_5)_3$. E.Y.C. acknowledges an Alfred P. Sloan Research Fellowship.

Supporting Information Available: Crystallographic data for **2**. This material is available free of charge via the Internet at http://pubs.acs.org.

References and Notes

(1) Butler, K.; Thomas, P. R.; Tyler, G. J. *J. Polym. Sci.* **1960**, *48*, 357−366.
(2) (a) Huang, S. S.; McGrath, J. E. *Polym. Prepr. (Am. Chem. Soc., Div. Polym. Chem.)* **1983**, *24*, 138−140. (b) Gia, H.; McGrath, J. E. *Polym. Bull. (Berlin)* **1980**, *2*, 837−840.
(3) Xie, X.; Hogen-Esch, T. E. *Macromolecules* **1996**, *29*, 1746−1752.
(4) (a) Kobayashi, M.; Ishizone, T.; Nakahama, S. *Macromolecules* **2000**, *33*, 4411−4416. (b) Kobayashi, M.; Okuyama, S.; Ishizone, T.; Nakahama, S. *Macromolecules* **1999**, *32*, 6466−6477.
(5) (a) Okamoto, Y.; Habaue, S.; Isobe, Y. In *Advances in Controlled/Living Radical Polymerization*; Matyjaszewski, K., Ed.; *ACS Symp. Ser.* **2003**, *854*, 59−71. (b) Isobe, Y.; Fujioka, D.; Habaue, S.; Okamoto, Y. *J. Am. Chem. Soc.* **2001**, *123*, 7180−7181.
(6) Lutz, J.-F.; Neugebauer, D.; Matyjaszewski, K. *J. Am. Chem. Soc.* **2003**, *125*, 6986−6993.
(7) Mariott, W. R.; Chen, E. Y.-X. *Macromolecules* **2004**, *37*, 4741−4743.
(8) (a) Stojcevic, G.; Kim, H.; Taylor, N. J.; Marder, T. B.; Collins, S. *Angew. Chem., Int. Ed.* **2004**, *43*, 5523−5526. (b) Lian, B.; Toupet, L.; Carpentier, J.-F. *Chem.—Eur. J.* **2004**, *10*, 4301−4307. (c) Ferenz, M.; Bandermann, F.; Sustmann, R.; Sicking, W. *Macromol. Chem. Phys.* **2004**, *205*, 1196−1205. (d) Karanikolopoulos, G.; Batis, C.; Pitsikalis, M.; Hadjichristidis, N. *J. Polym. Sci., Part A: Polym. Chem.* **2004**, *42*, 3761−3774. (e) Wang, J.; Odian, G.; Haubenstock, H. *Polym. Prepr. (Am. Chem. Soc., Div. Polym. Chem.)* **2003**, *44*, 673−674. Wang, J.; Haubenstock, H.; Odian, G. *Polym. Prepr. (Am. Chem. Soc. Div. Polym. Chem.)* **2003**, *44*, 675−676. (f) Bandermann, F.; Ferenz, M.; Sustmann, R.; Sicking, W. *Macromol. Symp.* **2001**, *174*, 247−253. (g) Karanikolopoulos, G.; Batis, C.; Pitsikalis, M.; Hadjichristidis, N. *Macromolecules* **2001**, *34*, 4697−4705. (h) Bandermann, F.; Ferenz, M.; Sustmann, R.; Sicking, W. *Macromol. Symp.* **2000**, *161*, 127−134. (i) Shiono, T.; Saito, T.; Saegusa, N.; Hagihara, H.; Ikeda, T.; Deng, H.; Soga, K. *Macromol. Chem. Phys.* **1998**, *199*, 1573−1579. (j) Li, Y.; Ward, D. G.; Reddy, S. S.; Collins, S. *Macromolecules* **1997**, *30*, 1875−1883. (k) Deng, H.; Shiono, T.; Soga, K. *Macromol. Chem. Phys.* **1995**, *196*, 1971−1980. (l) Collins, S.; Ward, S. G. *J. Am. Chem. Soc.* **1992**, *114*, 5460−5462. (m) Farnham, W. B.; Hertler, W. U.S. Pat. 4,728,706, 1988.
(9) (a) Bolig, A. D.; Chen, E. Y.-X. *J. Am. Chem. Soc.* **2004**, *126*, 4897−4906. (b) Strauch, J. W.; Fauré, J.-L.; Bredeau, S.; Wang, C.; Kehr, G.; Fröhlich, R.; Luftmann, H.; Erker, G. *J. Am. Chem. Soc.* **2004**, *126*, 2089−2104. (c) Chen, E. Y.-X.; Cooney, M. J. *J. Am. Chem. Soc.* **2003**, *125*, 7150−7151. (d) Karanikolopoulos, G.; Batis, C.; Pitsikalis, M.; Hadjichristidis, N. *Macromol. Chem. Phys.* **2003**, *204*, 831−840. (e) Batis, C.; Karanikolopoulos, G.; Pitsikalis, M.; Hadjichristidis, N.

Macromolecules **2003**, *36*, 9763−9774. (f) See ref 8e. (g) Bolig, A. D.; Chen, E. Y.-X. *J. Am. Chem. Soc.* **2002**, *124*, 5612−5613. (h) Frauenrath, H.; Keul, H.; Höcker, H. *Macromolecules* **2001**, *34*, 14−19. (i) Bolig, A. D.; Chen, E. Y.-X. *J. Am. Chem. Soc.* **2001**, *123*, 7943−7944. (j) Cameron, P. A.; Gibson, V.; Graham, A. J. *Macromolecules* **2000**, *33*, 4329−4335. (k) Stuhldreier, T.; Keul, H.; Höcker, H. *Macromol. Rapid Commun.* **2000**, *21*, 1093−1098. (l) Chen, Y.-X.; Metz, M. V.; Li, L.; Stern, C. L.; Marks, T. J. *J. Am. Chem. Soc.* **1998**, *120*, 6287−6305. (m) Deng, H.; Shiono, T.; Soga, K. *Macromolecules* **1995**, *28*, 3067−3073. (n) Soga, K.; Deng, H.; Yano, T.; Shiono, T. *Macromolecules* **1994**, *27*, 7938−7940. (o) Collins, S.; Ward, D. G.; Suddaby, K. H. *Macromolecules* **1994**, *27*, 7222−7224.

(10) (a) Saegusa, N.; Shiono, T.; Ikeda, T.; Mikami, K. JP 10330391, 1998. (b) Farnham, W. B.; Hertler, W. U.S. Pat. 4,728,706, 1988.

(11) (a) Jin, J.; Mariott, W. R.; Chen, E. Y.-X. *J. Polym. Chem., Part A: Polym. Chem.* **2003**, *41*, 3132−3142. (b) Jin, J.; Chen, E. Y.-X. *Organometallics* **2002**, *21*, 13−15.

(12) (a) Chen, E. Y.-X. *J. Polym. Sci., Part A: Polym. Chem.* **2004**, *42*, 3395−3403. (b) Jensen, T. R.; Yoon, S. C.; Dash, A. K.; Luo, L.; Marks, T. J. *J. Am. Chem. Soc.* **2003**, *125*, 14482−14494.

(13) (a) Rodriguez-Delgado, A.; Mariott, W. R.; Chen, E. Y.-X. *Macromolecules* **2004**, *37*, 3092−3100. (b) Jin, J.; Chen, E. Y.-X. *Macromol. Chem. Phys.* **2002**, *203*, 2329−2333. (c) Jin, J.; Wilson, D. R.; Chen, E. Y.-X. *Chem. Commun.* **2002**, 708−709. (d) Nguyen, H.; Jarvis, A. P.; Lesley, M. J. G.; Kelly, W. M.; Reddy, S. S.; Taylor, N. J.; Collins, S. *Macromolecules* **2000**, *33*, 1508−1510.

(14) (a) Hölscher, M.; Keul, H.; Höcker, H. *Macromolecules* **2002**, *35*, 8194−8202. (b) Hölscher, M.; Keul, H.; Höcker, H. *Chem.—Eur. J.* **2001**, *7*, 5419−5426. (c) Sustmann, R.; Sicking, W.; Bandermann, F.; Ferenz, M. *Macromolecules* **1999**, *32*, 4204−4213.

(15) Allen, R. D.; Long, T. E.; McGrath, J. E. *Polym. Bull. (Berlin)* **1986**, *15*, 127−134.

(16) (a) Grossman, R. B.; Doyle, R. A.; Buchwald, S. L. *Organometallics* **1991**, *10*, 1501−1505. (b) Collins, S.; Kuntz, B. A.; Taylor, N. J.; Ward, D. G. *J. Organomet. Chem.* **1988**, *342*, 21−29.

(17) Diamond, G. M.; Jordan, R. F.; Petersen, J. L. *J. Am. Chem. Soc.* **1996**, *118*, 8024−8033.

(18) Chen, E. Y.-X.; Kruper, W. J.; Roof, G.; Wilson, D. R. *J. Am. Chem. Soc.* **2001**, *123*, 745−746.

(19) Woodbury, R. P.; Rathke, M. W. *J. Org. Chem.* **1977**, *42*, 1688−1690.

(20) Rodriguez-Delgado, A.; Chen, E. Y.-X. *Macromolecules* **2005**, *38*, 2587−2594.

(21) (a) SMART, SAINT, and cell_now, Bruker Analytical X-ray Solutions, Madison, WI, 2001. (b) SHELXTL, Version 6.12; Bruker Analytical X-ray Solutions, Madison, WI, 2001.

(22) Spaether, W.; Klass, K.; Erker, G.; Zippel, F.; Fröhlich, R. *Chem.—Eur. J.* **1998**, *4*, 1411−1417.

(23) Klosin, J.; Roof, G. R.; Chen, E. Y.-X.; Abboud, K. A. *Organometallics* **2000**, *19*, 4684−4686.

(24) Horton, A. D.; de With, J.; van der Linder, A. J.; van de Weg, H. *Organometallics* **1996**, *15*, 2672−2674.

(25) Kodaira, T.; Tanahashi, H.; Hara, K. *Polym. J.* **1990**, *26*, 649−659.

(26) The P(DMAA)s produced from the chiral *ansa*-zirconocenium ester and amide enolates employed in this study exhibit no measurable [*mr*] + [*rr*] triad sequences from ^{13}C NMR spectra and are essentially stereodefect free within this detection limit ([*mm*] > 99%, Chart 1). For this reason, we could not directly determine, on the basis of spectroscopic data available, whether this polymerization is enantiomorphic-site or chain-end controlled. In addition, the [*mr*] and [*rr*] sequences in the carbonyl carbon region of lower tactic P(DMAA) samples produced by other initiators are not well-resolved. However, we have previously determined that, using the P(MMA)s by the chiral enolate **1**, which show a small amount of stereodefects suitable for such an analysis, the polymerization is enantiomorphic-site controlled.[20] Because methacrylate and acrylamide polymerizations by these chiral *ansa*-zirconocenium enolates proceed via essentially the same mechanisms (monometallic, intramolecular coordinative-conjugation addition) and because the P(DMAA) produced by an achiral analogue, $Cp_2Zr^+(THF)[OC(OEt)=CMe_2][MeB(C_6F_5)_3]^-$, is virtually atactic ([*m*]/[*r*] = 58/42]), we conclude that the polymerization of DMAA by chiral *ansa*-zirconocenium enolates is most likely enantiomorphic-site controlled.

MA051061Q